

Application of Ultrasonic Irradiation in Aqueous Synthesis of Highly Fluorescent CdTe/CdS Core–Shell Nanocrystals

ChunLei Wang,[†] Hao Zhang,^{†,‡} JunHu Zhang,[†] MinJie Li,[†] HaiZhu Sun,[†] and Bai Yang^{*,†}

Key Laboratory for Supramolecular Structure and Materials, College of Chemistry, Jilin University, Changchun 130012, People's Republic of China, and Max Planck Institute of Colloids and Interfaces, 14424 Potsdam, Germany

Received: October 8, 2006; In Final Form: December 4, 2006

1-Thioglycerol-capped CdTe nanocrystals were used as core template to generate CdTe/CdS core–shell nanocrystals in aqueous solution by means of ultrasonic irradiation. The photoluminescence quantum yields of CdTe/CdS core–shell nanocrystals were up to 20%, larger than the original CdTe nanocrystals by around 10 times. The reaction conditions, such as the concentration, the molar ratio of reactants, and the pH value, were investigated, showing that ultrasonic irradiation controlled the decomposition of thiourea and the formation of a gradient CdS shell around the original CdTe core.

Introduction

Semiconductor nanocrystals have attracted a great deal of attention due to their unique size-dependent optical properties. Capping nanocrystals with heterogeneously organic or inorganic shells is an efficient strategy to optimize their photoluminescence (PL) quantum yields (QYs), surface functionality, and robust photochemical stability, which are prerequisite for nanocrystal applications in bioimaging,¹ multicolour optical coding,² and optoelectronic devices.³ Up to now, the main efforts have been devoted to synthesis of various core–shell nanocrystals, such as CdSe/CdS, CdSe/ZnS, CdSe/ZnSe, CdTe/CdSe, CdTe/ZnS, CdS/ZnS, ZnSe/ZnS, PbSe/PbS, InP/ZnS, InAs/CdSe,^{4–13} and to investigate the influence of different shell materials on the emission properties of these nanocrystals. The prevalent viewpoint is that it requires a lattice matching between shells and core materials to achieve a better passivation and minimize the structure defects.¹⁴ In addition, the shells should have larger electronic band gap than the core to obtain higher QYs. Generally, proper shell capping can increase the QYs of nanocrystals for several to tens of times.

Nonetheless, almost all core–shell nanocrystals are synthesized by thermal decomposition of the organometallic precursors in organic media. Aqueous synthesis of core–shell nanocrystals is less reported. As compared with the organic one,^{4–13} aqueous synthesis of nanocrystals is more reproducible, cheaper, and less toxic. The hydrophilicity of the products holds a great promise in biological application. Recently, aqueous synthesis allows formation of CdTe nanocrystals with the QYs as high as 30–80% by appropriate surface modification or illumination.¹⁵ However, such CdTe nanocrystals can only be obtained by using mercaptocarboxylic acid as the ligand because the decomposition of mercaptocarboxylic acid leads to the formation of core–shell structure. For other ligand-capped nanocrystals, such as 1-thioglycerol (TG)-modified CdTe nanocrystals, whose hydroxyl groups are important for H-bond assembly and biosimulation,¹⁶ there still lacks an effective method to improve their

PL QYs (typically 1–1.5%, and 3% maximum¹⁷). Therefore, it should be desirable to develop new methods for preparing highly fluorescent core–shell nanocrystals with hydroxyl modification.

With the development of sonochemical technique,¹⁸ this approach has been widely used for preparation of various nanosized materials, such as carbides, oxides, sulfides, and composite nanoparticles.¹⁹ The products show unusual photoelectric and magnetic properties. The chemical effect of ultrasound originates from acoustic cavitation within collapsing bubbles, which generates localized hot spots with an exceedingly high transient temperature (5000 K), pressure (1800 atm), and cooling rate (10^{10} K/s).²⁰ Under this extreme condition, chemical reactions such as oxidation, reduction, dissolution, and decomposition can occur. Even some reactions, which are previously difficult to realize by other methods, can also proceed by using ultrasonic irradiation. In this work, ultrasonic irradiation was employed to aqueous synthesis of CdTe/CdS core–shell nanocrystals by using preformed TG-capped CdTe nanocrystals as template cores and thiourea as the sulfur source. It was found that ultrasound facilitated the decomposition of thiourea, leading to the formation of gradient CdS shell on CdTe cores. The resultant core–shell nanocrystals presented dramatically improved PL QYs, 10 times higher than the original nanocrystals.

Experimental Section

Materials. CdCl₂, NaBH₄, cadmium acetate, and thiourea were AR reagents from the Beijing Chemical Factory, China. TG was purchased from Aldrich.

Synthesis of CdTe Nanocrystals. CdTe nanocrystals were prepared according to the previous method.²¹ Typically: freshly prepared NaHTe solution was injected into the solution of CdCl₂ and TG after degassing with N₂ for 30 min at pH 9.5. The concentration of CdCl₂ was 1.25×10^{-3} mol/L, and the molar ratio of Cd²⁺/TG/Te²⁻ was 1:2.4:0.2. The crude solution was refluxed at 100 °C for 10 h to obtain CdTe nanocrystals. The calculated number of CdTe nanocrystals in solution is 10^{-5} – 10^{-6} mol·particles/L.

Synthesis of CdTe/CdS Nanocrystals. CdTe/CdS nanocrystals were prepared by ultrasonic irradiation. Typically, 3.25

* To whom correspondence should be addressed. E-mail: byangchem@jlu.edu.cn. Telephone: +86-431-5168478. Fax: +86-431-5193423.

[†] Jilin University.

[‡] Max Planck Institute of Colloids and Interfaces.

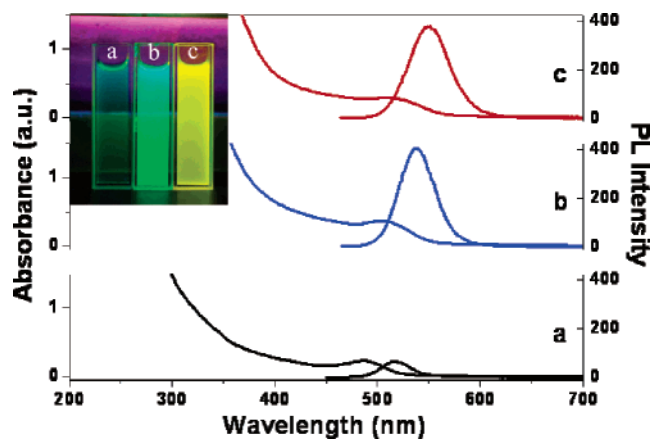


Figure 1. UV-vis absorption and PL spectra ($\lambda_{\text{ex}} = 400$ nm) of original TG-capped CdTe nanocrystals (a) and CdTe/CdS nanocrystals obtained by 2 h (b) and 4 h (c) ultrasound irradiation. Inset: PL images of the original TG-capped CdTe (a) and CdTe/CdS nanocrystals (b and c).

$\times 10^{-4}$ mol of cadmium acetate, 3.25×10^{-4} mol of thiourea, and 50 mL of freshly prepared TG-capped CdTe solution with pH 9.5–10.5 were mixed in a flask and bubbled with N_2 for 15 min, and then the flask was sealed and irradiated by ultrasound (KQ3200B ultrasonic base, 40 kHz, 150 W, purchased from Kunshan Ultrasonic Instrument Co., Ltd.) for several hours. The temperature of the reaction mixture rose to 80 °C during the ultrasonic irradiation. Any insoluble products were separated by centrifugation, and the supernatant was used for characterization. The influence of reactant concentration was tested by changing the amount of additional cadmium acetate and thiourea. X-ray powder diffraction (XRD) and X-ray photoelectron spectroscopy (XPS) characterization was carried out with the powder of CdTe and CdTe/CdS. To obtain such powder, CdTe and CdTe/CdS solutions were separated by centrifugation after adding isopropyl alcohol and then drying in the vacuum desiccator.

Characterization. UV-vis absorption spectra were recorded with a Shimadzu 3100 UV-vis-near-infrared spectrophotometer. Fluorescence experiments were performed with a Shimadzu RF-5301 PC spectrofluorimeter. XRD investigation was carried out using Siemens D5005 diffractometer. XPS was investigated by using a VG ESCALAB MK II spectrometer with a Mg K α excitation (1253.6 eV). Binding energy calibration was based on C 1s at 284.6 eV.

Results and Discussion

Fluorescence of CdTe/CdS Nanocrystals. CdTe/CdS nanocrystals are prepared through ultrasound irradiation of TG-capped CdTe nanocrystals in the presence of additional cadmium acetate and thiourea. During the ultrasonic irradiation, the color of the CdTe solution gradually changes from green to orange. Figure 1 presents the typical UV-vis absorption and PL spectra ($\lambda_{\text{ex}} = 400$ nm) of the original CdTe nanocrystals and the CdTe/CdS nanocrystals obtained by using ultrasound irradiation. The corresponding PL images are also shown in the inset picture. In comparison with the original CdTe nanocrystals (Figure 1a), CdTe/CdS nanocrystals show bright emission with an obvious red shift of spectra (Figure 1b,c). By using quinine in aqueous 0.5 mol/L H_2SO_4 as PL reference,²² the PL QYs of CdTe/CdS nanocrystals are evaluated as 20%. In contrast, the PL QYs of original TG-capped CdTe nanocrystals are merely 1–1.5%. The dramatic increase of QYs and the red shift of spectra are typical characteristics of core-shell nanocrystals, originating from the efficiently diminishing of the surface defects of core nanocrystals

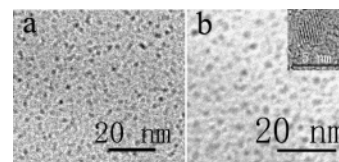


Figure 2. TEM images of the original TG-capped CdTe (a) and CdTe/CdS nanocrystals obtained by 2 h ultrasound irradiation (b). Inset: HRTEM image of one CdTe/CdS nanocrystal.

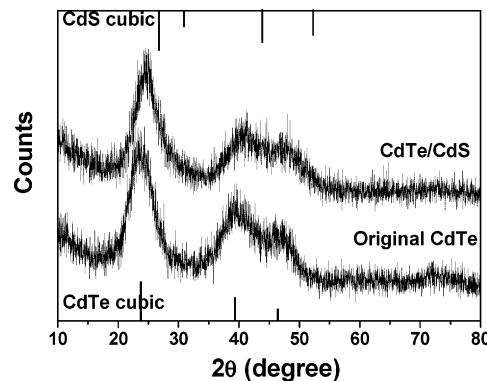


Figure 3. XRD patterns of the freshly prepared TG-capped CdTe nanocrystals and CdTe/CdS nanocrystals.

and the lowering of confinement energy of exciton after capping core nanocrystals with higher band gap shells.^{4–13}

CdTe/CdS Nanocrystals with Gradient CdS Shell. The diameters of TG-capped CdTe and CdTe/CdS nanocrystals are 2.5 and 2.8 nm calculated from UV-vis absorption spectra (Figure 1a,b).²³ The increased particle size might imply the formation of core-shell structure, since TG-capped CdTe nanocrystals have indicated dramatically slow growth rate at the same reaction period, making little variation in their UV-vis spectra.²¹ Transmission electron micrograph (TEM) images further reveal the increase of the size of CdTe/CdS nanocrystals (Figure 2). From the high-resolution TEM image of CdTe/CdS nanocrystals (inset of Figure 2b), no obvious lattice mismatch was observed, indicating the poor interface between the CdTe core and the CdS shell. According to the previous works,^{17,21,24} we deduce that the shell is a gradient layer varied from the core CdTe to a CdS-rich surface. Moreover, in our work, the core nanocrystals are directly used to prepare core-shell nanocrystals without any purification. Such condition benefits the simultaneous growth of core nanocrystals in the process of shell growth, thus leading to the formation of alloyed shells. As reported in the literature,^{24b} such an alloyed shell usually shows no abrupt boundary between the core and shell.

The formation of CdS shell is further characterized by XRD and XPS investigations. Figure 3 reveals the XRD patterns of freshly prepared TG-capped CdTe nanocrystals and CdTe/CdS core-shell nanocrystals. The broad diffractive peaks are typical for nanoparticles. The original CdTe nanocrystals show a cubic zinc blende structure, represented by the diffractive peaks at 23.5, 39.1, and 46.5°. While the CdTe/CdS nanocrystals show three obvious diffractive peaks at 24.5, 40.9, and 48.1, which are intermediate between the original CdTe and the cubic CdS phase. No separate CdS peaks are observed. Similar XRD results have been reported by the previous works,^{4b,15a,17,24} in which the nanocrystals possess gradient core-shell structures. Since XPS is powerful for identifying the compositions and structures of the surface of nanosized materials,²⁵ it is used to characterize the core-shell nature of CdTe/CdS nanocrystals. As shown in Figure 4, the binding energies of 572.8, 405.6, and 162.8 eV respectively correspond to the Te 3d, Cd 3d, and S 2p levels.

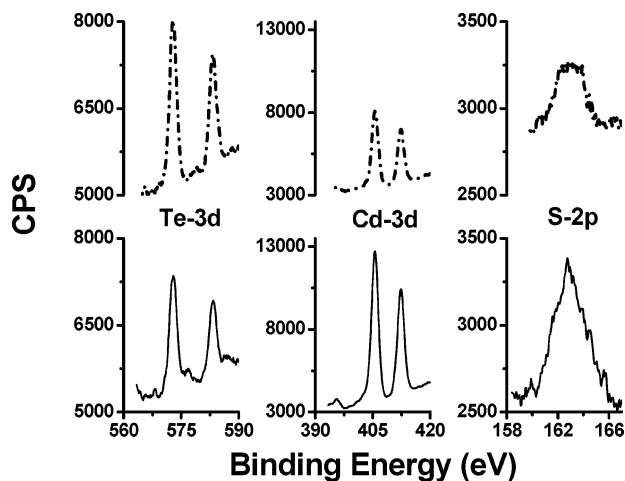


Figure 4. XPS data of the original TG-capped CdTe (top) and CdTe/CdS (bottom) nanocrystals. From left to right, the spectra are Te 3d, Cd 3d, and S 2p, respectively.

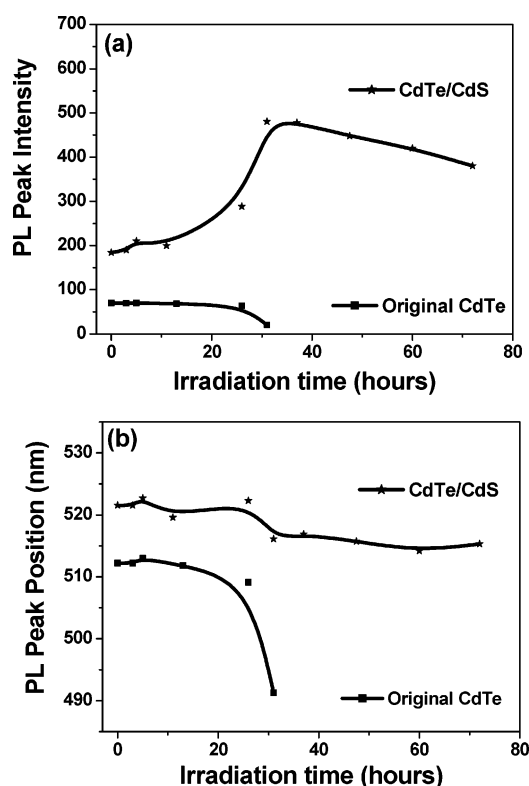


Figure 5. Variation profile of the PL peak intensity (a) and peak position (b) for the original TG-capped CdTe and CdTe/CdS nanocrystals under UV irradiation. The UV lamp is 40 W, and the wavelength is 365 nm.

Compared with the original CdTe ones, the resulting CdTe/CdS nanocrystals possess relatively high content of cadmium and sulfur and relatively low content of tellurium on their surface, indicating the existence of CdS-rich shells.

As suggested in the literature, photochemical stability of nanocrystals is one of the critical issues for their optical applications. A compact shell of either inorganic⁴⁻¹³ or organic material²⁶ is expected to improve their photochemical stability. Herein, we also compare the photochemical stability of CdTe and CdTe/CdS nanocrystals. Figure 5 shows the variation profile of PL peak intensity and peak position of the original CdTe and CdTe/CdS nanocrystals under ultraviolet irradiation. The dramatic reduction of PL intensity and evident blue shift of the PL peak were observed for CdTe nanocrystals, indicating the

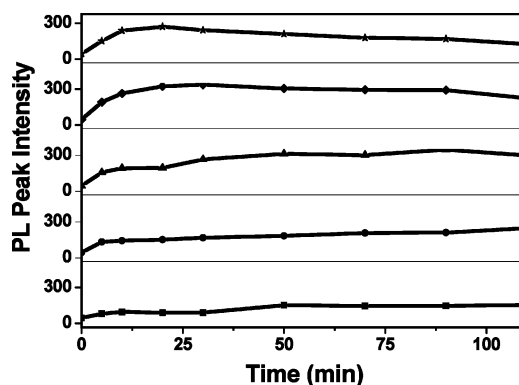


Figure 6. Variation profile of the PL peak intensity versus the reaction time with different concentrations of reactants. The concentration of cadmium acetate is equal to the one of thiourea. From bottom to top, the concentrations are 1.3×10^{-3} , 2.6×10^{-3} , 6.5×10^{-3} , 1.3×10^{-2} , and 1.95×10^{-2} mol/L.

photoinduced decomposition of nanocrystals (Figure 5).^{26c} After 30 h of irradiation, the PL almost vanished and macroscopic aggregates formed. In contrast, the CdTe/CdS nanocrystals showed improved stability against UV irradiation. In the initial stage during irradiation, the nanocrystal PL slightly increased due to the diminution of defects.^{17,27} Afterward, the PL intensity and peak position remained (Figure 5). The improved photochemical stability of the CdTe/CdS nanocrystals further demonstrated the formation of core-shell structure.

Influence of Experimental Variables. The success of our strategy strongly depends on the experimental conditions. Figure 6 shows the variation profile of the PL peak intensity versus the time of ultrasonic irradiation. Fixing the molar ratio of cadmium acetate and thiourea at 1:1, the concentration of cadmium acetate altered from 1.3×10^{-3} to 1.95×10^{-2} mol/L. During the reaction, the color of the solution changed to orange more rapidly for the samples with higher concentration of reactants, revealing a fast growth rate of the CdS shell. As shown in Figure 6, a maximum PL intensity was observed for each sample, reflecting the existence of an optimal thickness of the CdS shell in this reaction system. When the shell became thicker, the PL would in return decrease. Previous work also reported a similar result that was attributed to the formation of misfit dislocations due to the interface strain accumulation with the increased thickness of the shell.²⁸

Figure 7 indicates the PL spectra of CdTe/CdS nanocrystals with different molar ratios of cadmium acetate and thiourea under ultrasonic irradiation. Keeping cadmium acetate at the concentration of 6.5×10^{-3} mol/L, the concentration of thiourea changed from 1.6×10^{-3} to 1.3×10^{-2} mol/L. The samples possessing more thiourea show a much larger red shift of the PL peak than others within the same reaction period (Figure 7a). Moreover, we also found that the samples with more thiourea reached their highest PL intensity more rapidly (Figures 6 and 7). These results indicate the formation of the CdS shell depends mainly on the rate of the decomposition of thiourea. Compared with the profile of PL intensity (Figure 7b), it could be found that when the maximal PL intensity of the samples appeared, their peak position was near 530 nm, implying the optimal shell thickness had no relation with the ratio of reactants.

Figure 8 presents the pH effect on the PL of core-shell nanocrystals. When CdTe/CdS nanocrystals were prepared at relative high pH, they reached the highest PL intensity much faster. This pH-dependent effect should be attributed to the different decomposition products of thiourea. In alkaline condition, the decomposition product was S^{2-} and they would easily

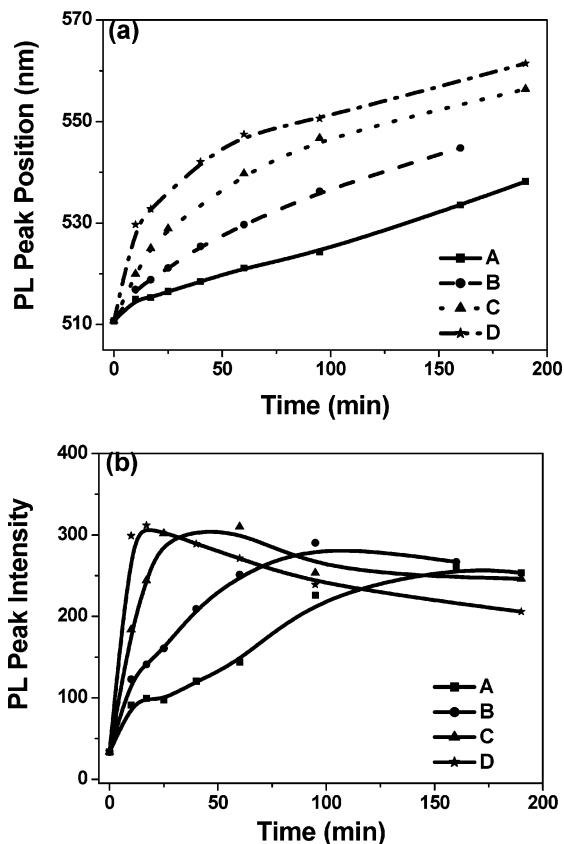
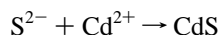


Figure 7. Variation profile of the PL peak position (a) and the peak intensity (b) versus the reaction time with different molar ratios of reactants. The concentration of cadmium acetate is 6.5×10^{-3} mol/L, and the concentrations of thiourea are 1.6×10^{-3} (A), 3.2×10^{-3} (B), 6.5×10^{-3} (C), and 1.3×10^{-2} mol/L (D).

react with cadmium acetate to form insoluble CdS. In contrast, at basic and acid conditions, the decomposition product was H_2S and it needed a deprotonation process before the formation of CdS.

In this work, we prepared aqueous CdTe/CdS nanocrystals by utilizing a sonochemical method. In fact, previous reports have revealed the ultrasonic decomposition of thiourea through the following process:²⁹



The radicals induced by ultrasonic irradiation accelerated the decomposition of thiourea. From Figures 6 and 7, the samples with more thiourea could produce more S^{2-} in the same period of ultrasonic irradiation, thus more rapidly reaching their highest PL intensity than others. Therefore, ultrasonic irradiation controlled the decomposition of thiourea and the formation of the CdS shell. Thus, highly luminescent CdTe/CdS core-shell nanocrystals were obtained. Note that H_2S was also used as an alternative S source for the preparation of CdTe/CdS core-shell nanocrystals under ultrasonic irradiation. Although obvious PL enhancement was observed, such enhancement was dramatically weaker than the one using thiourea as the S source. This difference should be attributed to the gradual decomposition of thiourea, facilitating a slow and uniform release of H_2S in the solution. It benefited the formation of homogeneous CdS on the surface of CdTe. In contrast, directly injecting H_2S into the

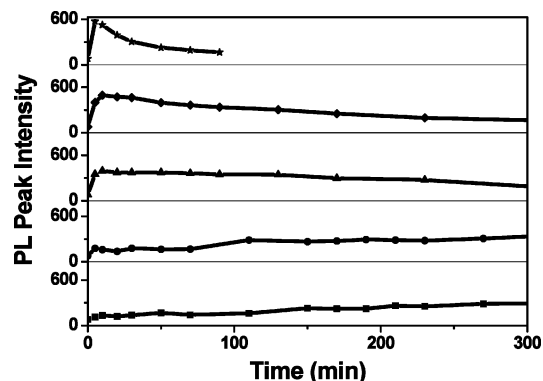


Figure 8. PL peak intensity versus the reaction time with different pH values. From bottom to top, the values are pH 8.01, 8.87, 9.44, 10.18, and 11.19.

reaction mixture made a rapid reaction between H_2S and Cd^{2+} ions, only leading to the formation of an unhomogeneous shell on CdTe nanocrystals, and hence the limited PL enhancement.

We chose TG-capped CdTe as the core template rather than mercaptocarboxylic acid capped nanocrystals by reason that the interaction between carboxyl groups and metal cations was too strong to achieve a stable mixture. When metal cations, such as Cd^{2+} and Zn^{2+} , were added into the solution, macroscopic aggregation that was induced by the interaction between carboxylic acid and metal cations made it difficult to prepare core-shell nanocrystals. This disadvantage was why less success was achieved in aqueous synthesis of core-shell nanocrystals. In contrast, hydroxyl-terminated CdTe nanocrystals had no such problem, and they could be used as the core template for the subsequent process of preparing core-shell nanocrystals.^{21b}

The small lattice mismatch together with the large band gap made CdS an ideal shell material for coating CdTe nanocrystals.¹⁴ Besides, the much smaller solubility of CdTe than CdS made sure that the tellurium in CdTe nanocrystals could not be substituted in the reaction process. However, the deposition process of CdS on the CdTe core was very slow. The simultaneous growth of CdTe nanocrystals during the process of shell growth led to the formation of only a gradient CdS shell. This process was quite like the formation of alloyed $\text{CdSe}_{1-x}\text{Te}_x$ nanocrystals.²⁴ The smaller solubility of CdTe than CdS made sure the faster formation of CdTe in the initial period of shell formation process. With the depleting of Te^{2-} , CdS dominated the shell growth and allowed the shell to form; thus highly luminescent CdTe/CdS nanocrystals were obtained. It also confirmed the gradient shell benefited to obtain nanocrystals with better shell coverage and higher QYs,³⁰ which was consistent with our experiment results.

Conclusions

Water-soluble CdTe/CdS core-shell nanocrystals with hydroxyl modification, high PL QYs (up to 20%), and improved photochemical stability were synthesized through the method of ultrasonic irradiation. Sonochemical condition facilitated the gradual decomposition of thiourea and uniform release of H_2S , thus favoring the homogeneous formation of a CdS shell on each CdTe core. Besides, the growth of the CdS shell was accompanied with the growth of the CdTe core self, leading to the formation of a gradient CdS shell. In this context, our finding was also helpful in revealing the exact structure and the mechanism of PL enhancement of aqueous synthesized CdTe nanocrystals. Because of their high PL QYs and improved photochemical stability, these CdTe/CdS nanocrystals are

expected to be applicable in biology, optical coding, and optoelectronic devices.

Acknowledgment. We thank Dr. Dayang Wang (Max Planck Institute of Colloids and Interfaces, Golm) for helpful discussion. This work is supported by the Special Funds for Major State Basic Research projects (Grant No. 2002CB613401), the Program for Changjiang Scholars and Innovative Research Team in University (Grant No. IRT0422), and the National Science Foundation of China (Grant No. 20534040).

References and Notes

- (1) (a) Chan, W. C. W.; Nie, S. M. *Science* **1998**, *281*, 2016. (b) Alivisatos, A. P. *Science* **1998**, *281*, 2013. (c) Akerman, M. E.; Chan, W. C. W.; Laakkonen, P.; Bhatia, S. N.; Ruoslahti, E. *Proc. Natl. Acad. Sci. U. S. A.* **2002**, *99*, 12617.
- (2) (a) Gaponik, N.; Radtchenko, I. L.; Sukhorukov, G. B.; Weller, H.; Rogach, A. L. *Adv. Mater.* **2002**, *14*, 879. (b) Kuang, M.; Wang, D.; Bao, H.; Gao, M.; Mohwald, H.; Jiang, M. *Adv. Mater.* **2005**, *17*, 267.
- (3) (a) Mamedova, N. N.; Kotov, N. A.; Rogach, A. L.; Studer, J. *Nano Lett.* **2001**, *1*, 281. (b) Lee, J.; Sundar, V. C.; Heine, J. R.; Bawendi, M. G.; Jensen, K. F. *Adv. Mater.* **2000**, *12*, 1102. (c) Selvan, S. T.; Bullen, C.; Ashokkumar, M.; Mulvaney, P. *Adv. Mater.* **2001**, *13*, 985. (d) Willner, I.; Patolsky, F.; Wasserman, J. *Angew. Chem., Int. Ed.* **2001**, *40*, 1861.
- (4) (a) Xie, R.; Kolb, U.; Li, J. X.; Basche, T.; Mews, A. *J. Am. Chem. Soc.* **2005**, *127*, 7480. (b) Pan, D.; Wang, Q.; Jiang, S.; Ji, X.; An, L. *Adv. Mater.* **2005**, *17*, 176. (c) Hao, E.; Sun, H.; Zhou, Z.; Liu, J.; Yang, B.; Shen, J. *Chem. Mater.* **1999**, *11*, 3096. (d) Mekis, I.; Talapin, D. V.; Kornowski, A.; Haase, M.; Weller, H. *J. Phys. Chem. B* **2003**, *107*, 7454.
- (5) (a) Talapin, D. V.; Rogach, A. L.; Kornowski, A.; Haase, M.; Weller, H. *Nano Lett.* **2001**, *1*, 207. (b) Cumberland, S. L.; Hanif, K. M.; Javierm, A.; Khitrov, G. A.; Strouse, G. F.; Woessner, S. M.; Yun, C. S. *Chem. Mater.* **2002**, *14*, 1576. (c) Wang, H.; Nakamura, H.; Uehara, M.; Yamaguchi, Y.; Miyazaki, M.; Maeda, H. *Adv. Funct. Mater.* **2005**, *15*, 603.
- (6) Reiss, P.; Bleuse, J.; Pron, A. *Nano Lett.* **2002**, *2*, 781.
- (7) (a) Kim, S.; Fisher, B.; Eisler, H. J.; Bawendi, M. *J. Am. Chem. Soc.* **2003**, *125*, 11466. (b) Yu, K.; Zaman, B.; Romanova, S.; Wang, D. S.; Ripmeester, J. A. *Small* **2004**, *1*, 332.
- (8) Tsay, J. M.; Pflughoeft, M.; Bentolila, L. A.; Weiss, S. *J. Am. Chem. Soc.* **2004**, *126*, 1926.
- (9) (a) Steckel, J. S.; Zimmer, J. P.; Sullivan, S. C.; Stott, N. E.; Bulovic, V.; Bawendi, M. G. *Angew. Chem., Int. Ed.* **2004**, *43*, 2154. (b) Hsu, Y.; Lu, S.; Lin, Y. *Adv. Funct. Mater.* **2005**, *15*, 1350. (c) Yang, H.; Holloway, P. H. *Adv. Funct. Mater.* **2004**, *14*, 152.
- (10) (a) Nikesh, V. V.; Mahamuni, S. *Semicond. Sci. Technol.* **2001**, *16*, 687. (b) Chen, H. S.; Lo, B.; Hwang, J. Y.; Chang, G. Y.; Chen, C. M.; Tasi, S. J.; Wang, S. J. *J. Phys. Chem. B* **2004**, *108*, 17119.
- (11) Sashchiuk, A.; Langof, L.; Chaim, R.; Lifshitz, E. *J. Cryst. Growth* **2002**, *240*, 431.
- (12) Haubold, S.; Haase, M.; Kornowski, A.; Weller, H. *Chem. Phys. Chem.* **2001**, *2*, 331.
- (13) (a) Cao, Y. W.; Banin, U. *Angew. Chem., Int. Ed.* **1999**, *38*, 3692. (b) Cao, Y. W.; Banin, U. *J. Am. Chem. Soc.* **2000**, *122*, 9692.
- (14) Trindade, T.; O'Brien, P.; Pickett, N. L. *Chem. Mater.* **2001**, *13*, 3843.
- (15) (a) Bao, H.; Gong, Y.; Li, Z.; Gao, M. *Chem. Mater.* **2004**, *16*, 3853. (b) Gao, M.; Kirstein, S.; Mohwald, H.; Rogach, A. L.; Kornowski, A.; Eychmuller, A.; Weller, H. *J. Phys. Chem. B* **1998**, *102*, 8360.
- (16) (a) Gong, Y.; Gao, M.; Wang, D.; Mohwald, H. *Chem. Mater.* **2005**, *17*, 2648. (b) Kuther, J.; Seshadri, R.; Tremel, W. *Angew. Chem., Int. Ed.* **1998**, *37*, 3044.
- (17) (a) Gaponik, N.; Talapin, D. V.; Rogach, A. L.; Hoppe, K.; Shevchenko, E. V.; Kornowski, A.; Eychmuller, A.; Weller, H. *J. Phys. Chem. B* **2002**, *106*, 7177. (b) He, Y.; Lu, H.; Sai, L.; Lai, W.; Fan, Q.; Wang, L.; Huang, W. *J. Phys. Chem. B* **2006**, *110*, 13370.
- (18) (a) Suslick, K. *Science* **1990**, *247*, 1439. (b) Henglein, A. *Ultrasonics* **1987**, *25*, 6. (c) Einhorn, C.; Einhorn, J.; Luche, J. L. *Synthesis* **1989**, *11*, 787. (d) Kotronarou, A.; Mills, G.; Hoffmann, M. R. *J. Phys. Chem.* **1991**, *95*, 3630.
- (19) (a) Suslick, K.; Choe, S. B.; Cichowlas, A. A.; Grinstaff, M. W. *Nature* **1991**, *353*, 414. (b) Hyeon, T.; Fang, M.; Suslick, K. *J. Am. Chem. Soc.* **1996**, *118*, 5492. (c) Cao, X.; Koltypin, Y.; Katabi, G.; Felner, I.; Gedanken, A. *J. Mater. Res.* **1997**, *12*, 405. (d) Sostaric, J. Z.; Caruso-Hubson, R. A.; Mulvaney, P.; Grieser, F. *J. Chem. Soc., Faraday Trans.* **1997**, *93*, 1791. (e) Arul Dhas, N.; Gedanken, A. *Appl. Phys. Lett.* **1998**, *72*, 2511. (f) Vinodgopal, K.; He, Y.; Ashokkumar, M.; Grieser, F. *J. Phys. Chem. B* **2006**, *110*, 3849.
- (20) Suslick, K. S. *Ultrasound: Its Chemical, Physical and Biological Effects*; VCH: Weinheim, Germany, 1988.
- (21) (a) Rogach, A. L.; Katsikas, L.; Kornowski, A.; Su, D.; Eychmuller, A.; Weller, H. *Ber. Bunsen-Ges. Phys. Chem.* **1996**, *100*, 1772. (b) Harrison, M. T.; Kershaw, S. V.; Burt, M. G.; Eychmuller, A.; Weller, H.; Rogach, A. L. *Mater. Sci. Eng. B* **2000**, *355*, 69–70. (c) Zhang, H.; Wang, L.; Xiong, H.; Hu, L.; Yang, B.; Li, W. *Adv. Mater.* **2003**, *15*, 1712. (d) Zhang, H.; Zhou, Z.; Yang, B.; Gao, M. Y. *J. Phys. Chem. B* **2003**, *107*, 8. (e) Rogach, A. L. *Mater. Sci. Eng. B* **2000**, *435*, 69–70.
- (22) Talapin, D. V.; Rogach, A. L.; Shevchenko, E. V.; Kornowski, A.; Haase, M.; Weller, H. *J. Am. Chem. Soc.* **2002**, *124*, 5782.
- (23) (a) Pesika, N. S.; Stebe, K. J.; Searson, P. C. *Adv. Mater.* **2003**, *15*, 1289. (b) Rajh, T.; Micic, O. I.; Nozik, A. J. *J. Phys. Chem.* **1993**, *97*, 11999.
- (24) (a) Zhong, X.; Han, M.; Dong, Z.; White, T. J.; Knoll, W. *J. Am. Chem. Soc.* **2003**, *125*, 8589. (b) Bailey, R. E.; Nie, S. *J. Am. Chem. Soc.* **2003**, *125*, 7100.
- (25) (a) Borchert, H.; Haubold, S.; Haase, M.; Weller, H.; Meginley, C.; Riedler, M.; Moller, T. *Nano Lett.* **2002**, *2*, 151. (b) Zhang, H.; Yang, B. *Thin Solid Film* **2002**, *418*, 169. (c) Borchert, H.; Talapin, D. V.; Gaponik, N.; Meginley, C.; Adam, S.; Lobo, A.; Moller, T.; Weller, H. *J. Phys. Chem. B* **2003**, *107*, 9662.
- (26) (a) Guo, W.; Li, J.; Wang, Y.; Peng, X. *J. Am. Chem. Soc.* **2003**, *125*, 3901. (b) Wang, Y. A.; Li, J. T.; Chen, H.; Peng, X. *J. Am. Chem. Soc.* **2002**, *124*, 2293. (c) Aldana, J.; Wang, Y. A.; Peng, X. *J. Am. Chem. Soc.* **2001**, *123*, 8844.
- (27) Wang, Y.; Tang, Z.; Correa-Duarte, M. A.; Pastoriza-Santos, I.; Giersig, M.; Kotov, N. A.; Liz-Marzan, L. M. *J. Phys. Chem. B* **2004**, *108*, 15461.
- (28) Baranov, A. V.; Rakovich, Y. P.; Moore, R. A.; Talapin, D. V.; Rogach, A. L.; Masumoto, Y.; Nabiev, E. *Phys. Rev. B* **2003**, *68*, 165306.
- (29) (a) Dhas, N. A.; Zaban, A.; Gedanken, A. *Chem. Mater.* **1999**, *11*, 806. (b) Gao, T.; Li, Q. H.; Wang, T. H. *Chem. Mater.* **2005**, *17*, 887.
- (30) McBride, J.; Treadway, J.; Feldman, L. C.; Pennycook, S. J.; Rosenthal, S. J. *Nano Lett.* **2006**, *6*, 1496.